Cell Reports

Report

PARylation of BRCA1 limits DNA break resection through BRCA2 and EXO1

Graphical abstract

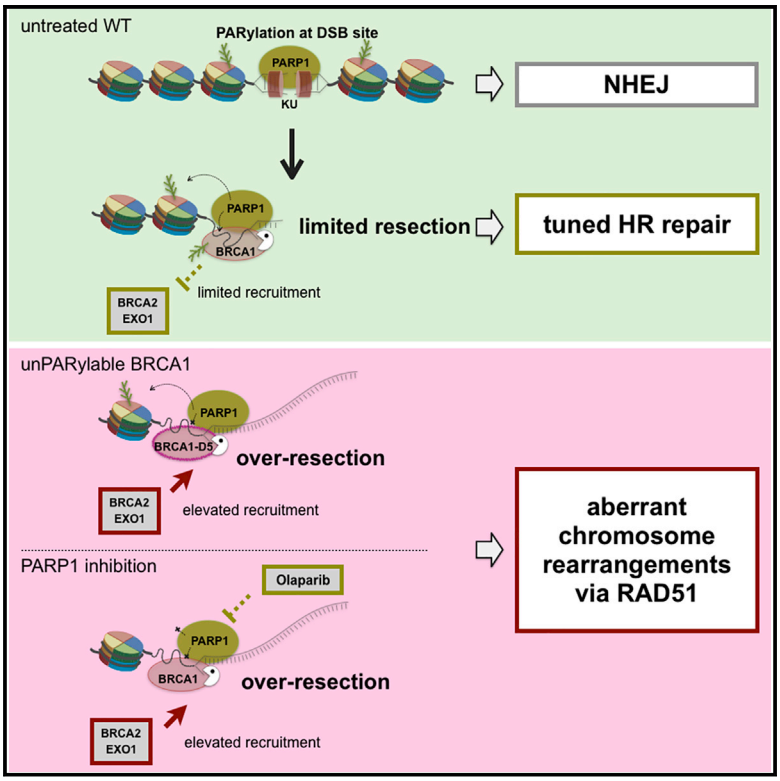

Highlights

- PARP1 inhibition leads to over-resection of Cas9-induced DNA double-strand breaks
- Downregulation of BRCA1 or BRCA2 abrogates excessive PARPi-dependent DNA resection
- Expression of unPARylable BRCA1 variant induces over-resection of Cas9-induced DSBs
- BRCA2 and EXO1 promotes DSB over-resection in unPARylable BRCA1 cells

Authors

Samuele Lodovichi, Roberto Quadri, Sarah Sertic, Achille Pellicioli

Correspondence

achille.pellicioli@unimi.it

In brief

Lodovichi et al. show that BRCA1 PARylation limits excessive resection of DNA double-strand breaks (DSBs). Inhibition of PARP1 or expression of an unPARylable variant of BRCA1 leads to over-resection of DSBs via the BRCA2/EXO1 axis, promoting RAD51-dependent DNA repair. These findings elucidate the mechanism of PARP inhibition in cancer therapy.

Lodovichi et al., 2023, Cell Reports *42*, 112060
February 28, 2023
https://doi.org/10.1016/j.celrep.2023.112060

CellPress

Cell Reports

CellPress
OPEN ACCESS

Report

PARylation of BRCA1 limits DNA break resection through BRCA2 and EXO1

Samuele Lodovichi,[1,2,3] Roberto Quadri,[1,3] Sarah Sertic,[1] and Achille Pellicioli[1,4,*]
[1]Dipartimento di Bioscienze, Università degli Studi di Milano, 20131 Milano, Italy
[2]Present address: Cancer Epidemiology Program, H. Lee Moffitt Cancer Center and Research Institute, 12902 Magnolia Drive, Tampa, FL 33612, USA
[3]These authors contributed equally
[4]Lead contact
*Correspondence: achille.pellicioli@unimi.it
https://doi.org/10.1016/j.celrep.2023.112060

SUMMARY

The nucleolytic processing (resection) of a DNA double-strand break (DSB) is a critical step to repair the lesion by homologous recombination (HR). PARylation, which is the attachment of poly(ADP-ribose) (PAR) units to specific targets by PAR polymerases (PARPs), regulates many steps of HR, including resection. Here, we show that preventing PARylation of the oncosuppressor BRCA1 induces hyper-resection of DSBs through BRCA2 and the EXO1 nuclease. Upon expression of the unPARylatable variant of BRCA1, we observe a reduced 53BP1-RIF1 barrier for resection accompanied by an increase in the recruitment of the RAD51 recombinase. Similar results are observed when cells are treated with the clinically approved PARP inhibitor olaparib. We propose that PARylation of BRCA1 is important to limit the formation of excessively extended DNA filaments, thereby reducing illegitimate chromosome rearrangements. Our results shed light on molecular aspects of HR and on the mechanisms of PARP inhibitor treatment.

INTRODUCTION

The poly(ADP-ribose) polymerase 1 (PARP1) gene codes for a nuclear protein that attaches a PAR polymer to itself and to other proteins involved in several aspects of cellular metabolism, including DNA repair.[1,2] PARP1, together with HPF1, is also responsible for serine ADP-ribosylation of histones and other proteins in different metabolic conditions including DNA damage.[3–8] PARP1 is engaged by double-strand breaks (DSBs), promoting recruitment of downstream effectors that determine the choice of DNA repair either by the error-free homologous recombination (HR) or the error-prone non-homologous end joining (NHEJ) pathways. The decision is finely regulated and depends on the nucleolytic processing of the DSB ends, a mechanism called DNA resection.[9]

Several proteins are involved in the regulation of DNA resection, which can be either promoted or limited, also depending on the cell-cycle phase. During G1 phase, suppressing resection is critical to drive DSB repair through NHEJ. One of the first factors recruited to the site of damage is the KU70/80 heterodimer, which binds the broken ends of the DNA, protecting them from nucleases. Similarly, RIF1 and 53BP1 oligomers assemble nearby the DSB through interaction with modified histones, TopBP1, and other proteins localized at the DNA lesion, acting as a scaffold that limits DSB resection.[10,11] Conversely, during S-G2 phase, DNA resection is stimulated, and HR is favored.[9]

Resection is carried out by the resectosome,[12] a dynamic protein machinery composed by several factors. The MRE11-RAD50-NBS1 (MRN) complex, in association with CtIP, nicks the DNA in proximity to the DSB, allowing a 3′-5′ nucleolytic degradation of DNA by MRE11 (short-range resection). Then, a sophisticated cooperation by the nucleases EXO1 and DNA2 determines extensive 5′-3′ degradation of DNA (long-range resection), leading to the formation of single-stranded (ss) DNA for recombination.[13] BRCA1 and BRCA2, two central proteins in HR and genome integrity in human cells, are also recruited early to DSBs, with BRCA1 being involved in controlling resectosome activity and BRCA2 in the nucleation of RAD51 oligomers on the ssDNA filament.[14,15] Notably, BRCA1 is ADP-ribosylated by PARP1,[4,16,17] and treatment with PARP inhibitors may interfere with DNA resection by (1) limiting early phase histone eviction from the break site,[18] (2) limiting early recruitment of NBS1[19,20] and EXO1[21,22] at DSBs, and (3) destabilizing the resection barrier factors KU70/80 and 53BP1-RIF1 nearby the break, also facilitating EXO1 and DNA2 activities for the long-range resection.[23] However, the molecular details of this regulation and the implication for cancer treatment are still poorly understood.

Different PARP inhibitors have been approved for cancer therapy by the US Food and Drug Administration (FDA) and the European Medicines Agency (EMA). In particular, they have shown promise in the treatment of certain types of breast and ovarian cancers deficient in BRCA1 or BRCA2 activity. Upon their administration, *BRCA1/2*-deficient cancer cells accumulate excessive DNA damage and eventually die.[24,25]

To elucidate the mechanism by which the inhibition of PARylation interferes with DNA resection, we utilized a system in which

inducible Cas9 endonuclease creates DSBs at specific target sequences.[26] We found that preventing BRCA1 PARylation, by olaparib treatment or specific BRCA1 mutation,[16] promotes EXO1- and BRCA2-dependent DSB resection and destabilizes RIF1-53BP1 oligomers at DSBs. These results extend current knowledge on resection mechanisms and may have implications for the use of PARP inhibitors in breast and ovarian cancer therapy.

RESULTS

PARP inhibition by olaparib promotes DSB over-resection through BRCA1 and BRCA2

Taking advantage of droplet digital PCR assay at DSB (ddPaD),[26] we quantified the amount of ssDNA formed at two DSBs induced by Cas9 in BRCA1- or BRCA2-silenced U-2OS cells, as outlined in Figure 1A. 72 h after silencing, cells were transfected with single guide RNAs (sgRNAs) to induce DSB1 and DSB2 and treated with olaparib 5 μM or DMSO (silencing control is shown in Figures S1A and S1B). Then, 6 h after sgRNA transfection, DNA was extracted and analyzed (Figure 1B). Inhibition of PARylation by olaparib led to a statistically significant increase in DNA resection at both DSB1 and DSB2 sites (Figure 1C), suggesting that PARP1 influences resection of Cas9-induced DSBs, as previously reported for other types of DSBs.[23] Interestingly, the increase of ssDNA generated by resection was significant at close distance from the DSB (335 bp from DSB1 and 364 bp from DSB2) (Figure 1C) and was also measurable at longer distance (1,618 bp from DSB1 and 1,754 bp from DSB2) (Figure S1C), suggesting that PARylation might affect both the short- and long-range resection steps of Cas9-induced DSBs. BRCA1 silencing strongly affected resection of Cas9-induced DSBs, independent of olaparib treatment (Figure 1C), while no statistically significant decrease in the amount of ssDNA at the breaks was observed in BRCA2-silenced cells (Figures 1C and S1C). The amount of ssDNA was slightly increased at DSB2 when BRCA2 was depleted when compared with control cells, particularly at the longer distance (Figure S1C), a discrepancy that has been already observed in other experimental conditions.[27] However, BRCA2 depletion limited the extended DNA resection induced by olaparib treatment at both DSB1 and DSB2 sites (Figures 1B, S1C, and S1D). These results indicate that the over-resection observed in olaparib-treated cells depends on BRCA1 and BRCA2. While the severe impairment in BRCA1-silenced cells is likely due to an inactive resectosome, the defect in BRCA2-silenced cells suggests a mechanism to inhibit over-resection by PARylation of key factors, including components of the resectosome itself.

UnPARylatable variant of BRCA1 affects RIF1, RAD51, and BRCA2 recruitment at DSBs

Next, we analyzed nuclear foci of proteins related to DSB processing in cells treated with the combination of the radiomimetic compound bleomycin and olaparib. We focused on cells in G2 phase (cyclin B1-positive staining), when DSB resection and HR repair are proficient. We found that the dual combination of bleomycin and olaparib reduced the foci of the anti-resection factor RIF1 when compared with cells treated with bleomycin only (Figure 2A). These results are in agreement with previous ones showing a reduction of RIF1 foci in PARP1-depleted cells treated with ionizing radiation[23] and are consistent with the increased resection of Cas9-induced DSBs by olaparib treatment (Figure 1).

On the other hand, foci of RAD51, which is recruited to ssDNA of resected DSBs to promote HR, increased in cells treated with bleomycin and olaparib (Figure 2B), further supporting that the inhibition of PARylation leads to higher amount of ssDNA by resection. Interestingly, formation of RAD51 foci upon DSBs induction is strongly affected by the depletion of either BRCA1 or CtIP with/without olaparib treatment (Figures S2A and S2B), suggesting that the resectosome may not be properly functional in these conditions. Noteworthy, the ectopic expression of a silencing-resistant BRCA1 from a plasmid restored the bleomycin-induced RAD51 foci formation in BRCA1-silenced cells (Figure S2A). We then analyzed RIF1 and RAD51 foci in cells depleted of HPF1, which cooperates with PARP1 to control recruitment of DNA repair factors at damaged chromatin.[28] Cells have been transfected with specific small interfering RNA (siRNA) against HPF1 (Figure S2C) and then treated with bleomycin to induce DSBs, as in Figure 2A. Our analyses show that formation of RIF1 foci decreased (Figure 2C) while RAD51 foci increased (Figure 2D) in HPF1-silenced cells, similarly to what we have found in olaparib-treated cells (Figures 2A and 2B). We conclude that ADP-ribosylation of target proteins mediated by PARP1 and HPF1 is fundamental to control recruitment of critical DNA repair factors at DSBs, also controlling the amount of ssDNA by resection.

To directly assess the role of PARP1 activity on the BRCA1/BRCA2 axis for DSB resection, we analyzed RIF1, RAD51, and BRCA2 foci in cells silenced for endogenous BRCA1 and expressing a silencing-resistant ectopic wild-type (WT) BRCA1 or the BRCA1-D5 variant that cannot be properly PARylated[16] (Figures 3A and S3A). In bleomycin-treated cells (Figure 3A), expression of BRCA1-D5 induced a reduction in RIF1 foci accompanied by an increase in RAD51 foci compared with cells expressing BRCA1-WT (Figures 3B and 3C). Although BRCA1 (WT or D5) has been ectopically expressed from a plasmid, the results obtained in Figures 3B and 3C are similar to what we have found in U-2OS cells expressing the endogenous BRCA1-WT and treated with the dual combination of bleomycin and olaparib (Figures 2, S2A, and S3A). Cells expressing BRCA1-D5 have also shown an increase of BRCA2 foci (Figure 3D), further supporting the elevated binding of RAD51. Interestingly, olaparib treatment did not have any additive effect on RIF1 or RAD51 foci formation in cells expressing the BRCA1-D5 variant (Figures S3B and S3C). Overall, these results show that BRCA1 and PARP1 cooperate to control DSB resection and that BRCA1 PARylation is critical to modulate the recruitment of RIF1, RAD51, and BRCA2 near a DSB.

UnPARylatable variant of BRCA1 increases DSB resection through BRCA2 and EXO1

Based on the obtained results, we hypothesized that expression of the unPARylatable BRCA1-D5 variant might trigger elevated DSB resection comparable to olaparib treatment. To address

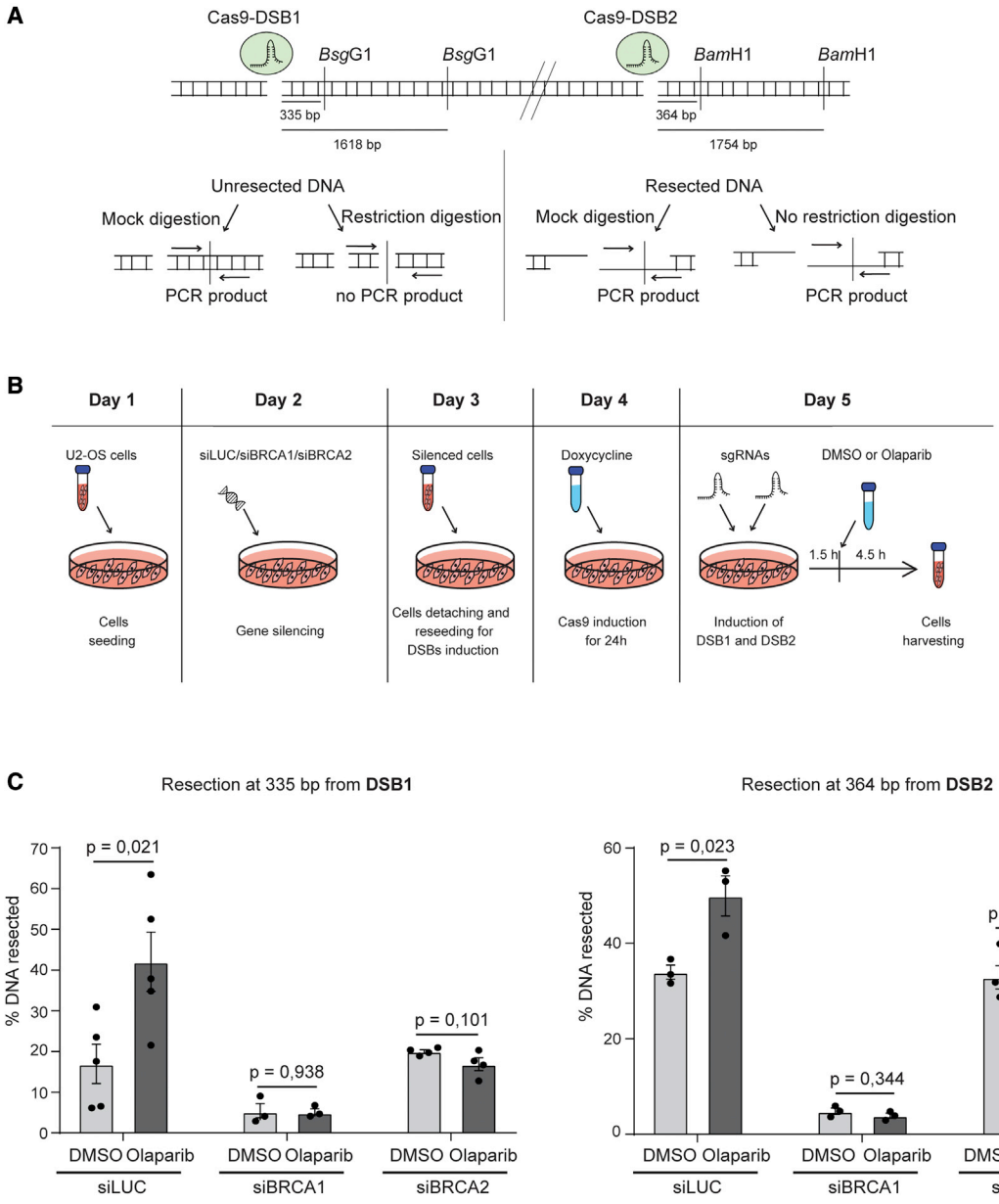

Figure 1. Treatment with olaparib triggers DNA hyper-resection at Cas9-induced DSBs through BRCA1 and BRCA2

(A) Experimental approach to analyze the formation and processing of DSB1 and DSB2 in U-2OS-SEC (stably expressing Cas9) cells. Specific oligonucleotides were designed to quantify ssDNA at the indicated distance from the DSBs (Table S1). The two DSBs are induced simultaneously by transfection with sgRNA1 and sgRNA2. Genomic DNA is extracted and digested with given restriction enzymes at specific distances from the DSB. If the target sequence has been converted into ssDNA by the resection started at the DSB, it cannot be digested by the restriction enzyme, and the DNA will be amplified by the ddPCR. A region on chromosome 22 that is not cut by these enzymes served as control. Values indicating the percentage of cutting efficiency, exposed ssDNA, and resected DSB were calculated as described previously.[26]

(B) Experimental pipeline for experiment in (C). U-2OS cells are transfected with siRNAs targeting either BRCA1 or BRCA2 (siLUC is also used as negative control). The next day, cells are detached and seeded again in the presence of doxycycline to induce Cas9 expression. On day 5, cells are transfected with sgRNA1 and sgRNA2 to induce DSB1 and DSB2. 1.5 h after sgRNA transfection, cells are treated with 5 μM olaparib or DMSO (vehicle).

(C) Percentage of DNA resected at DSB1 and DSB2 by ddPCR analysis in BRCA1- or BRCA2-depleted cells. Data are plotted as mean ± SEM, and a t test has been performed to analyze statistical difference among means calculated from at least three biological replicates; p values obtained from this analysis are shown. Cut efficiency DSB1: siLUC (DMSO) = 47.75% ± 50%; siLUC (olaparib) = 46.86% ± 7.05%; siBRCA1 (DMSO) = 52.96% ± 2.85%; siBRCA1 (olaparib) = 54.43% ± 2.52%; siBRCA2 (DMSO) = 37.52% ± 3.47%; siBRCA2 (olaparib) = 39.69% ± 4.87%. Cut efficiency DSB2: siLUC (DMSO) = 42.19% ± 4.63%; siLUC (olaparib) = 42.38% ± 6.97%; siBRCA1 (DMSO) = 49.37% ± 1.97%; siBRCA1 (olaparib) = 49.92% ± 1.12%; siBRCA2 (DMSO) = 42.02% ± 4.98%; siBRCA2 (olaparib) = 39.47% ± 5.09%.

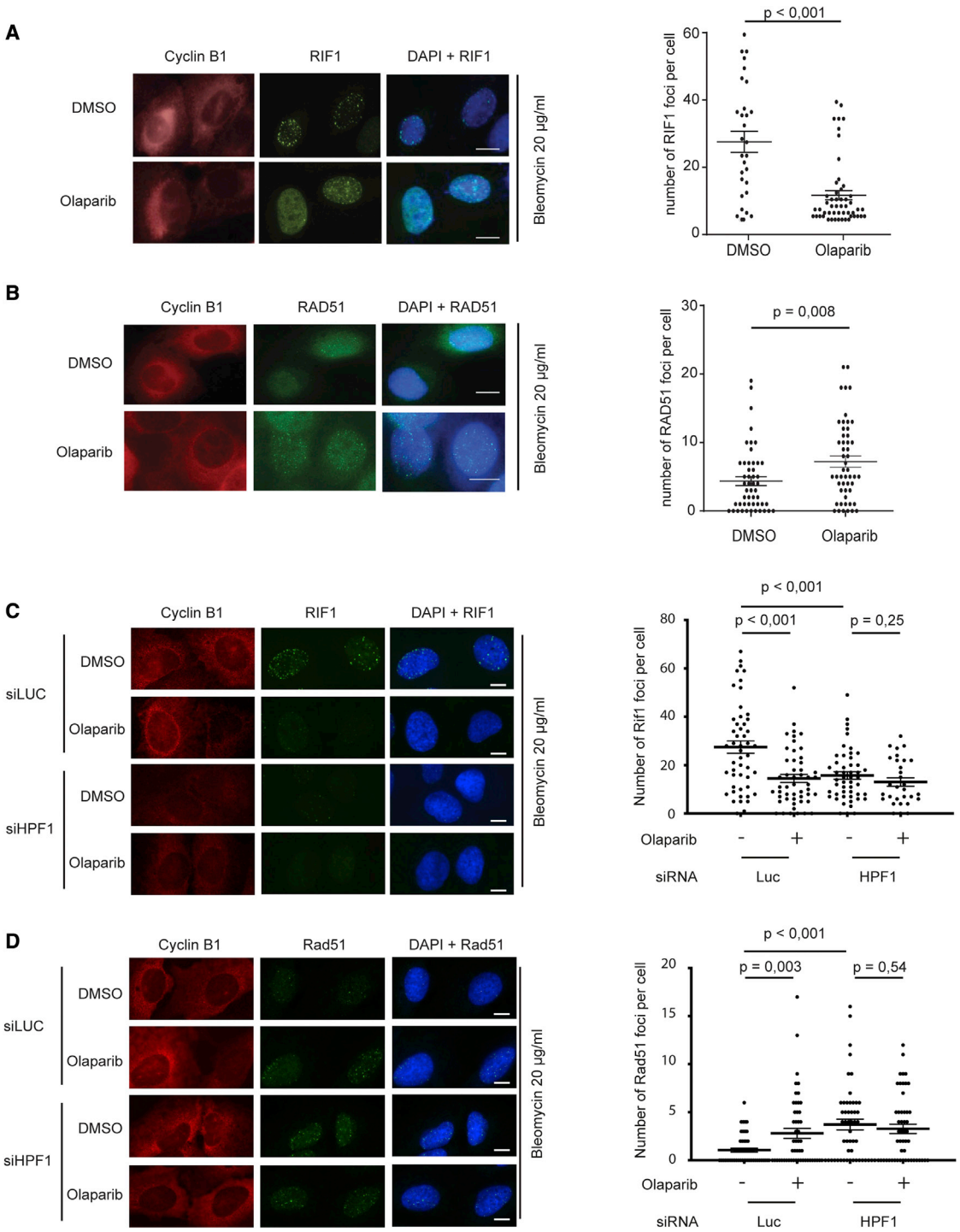

Figure 2. Treatment with olaparib or HPF1 silencing reduces the recruitment at DSBs of the DNA resection inhibitor RIF1, while it increases the recruitment of the HR factor RAD51

(A and B) U-2OS cells were treated for 3 h with bleomycin 20 μg/mL or DMSO (vehicle).

(C and D) U-2OS cells were transfected with control or HPF1-directed siRNAs and, after 48 h, treated for 3 h with bleomycin 20 μg/mL or DMSO (vehicle); silencing controls are reported in Figure S2C.

Cells were then fixed and analyzed by immunofluorescence microscopy with specific antibodies directed against RIF1 (A and C) or RAD51 (B and D). Ciclyn-B1 was analyzed to discriminate cells in S-G2 phase. Left: representative images of cells. Scale bars: 10 μm. Right: foci number per cell; a t test was performed to analyze statistical difference between means calculated counting foci in at least 50 cells per experiment (n = 3, biologically independent experiments); p values obtained from this analysis are shown.

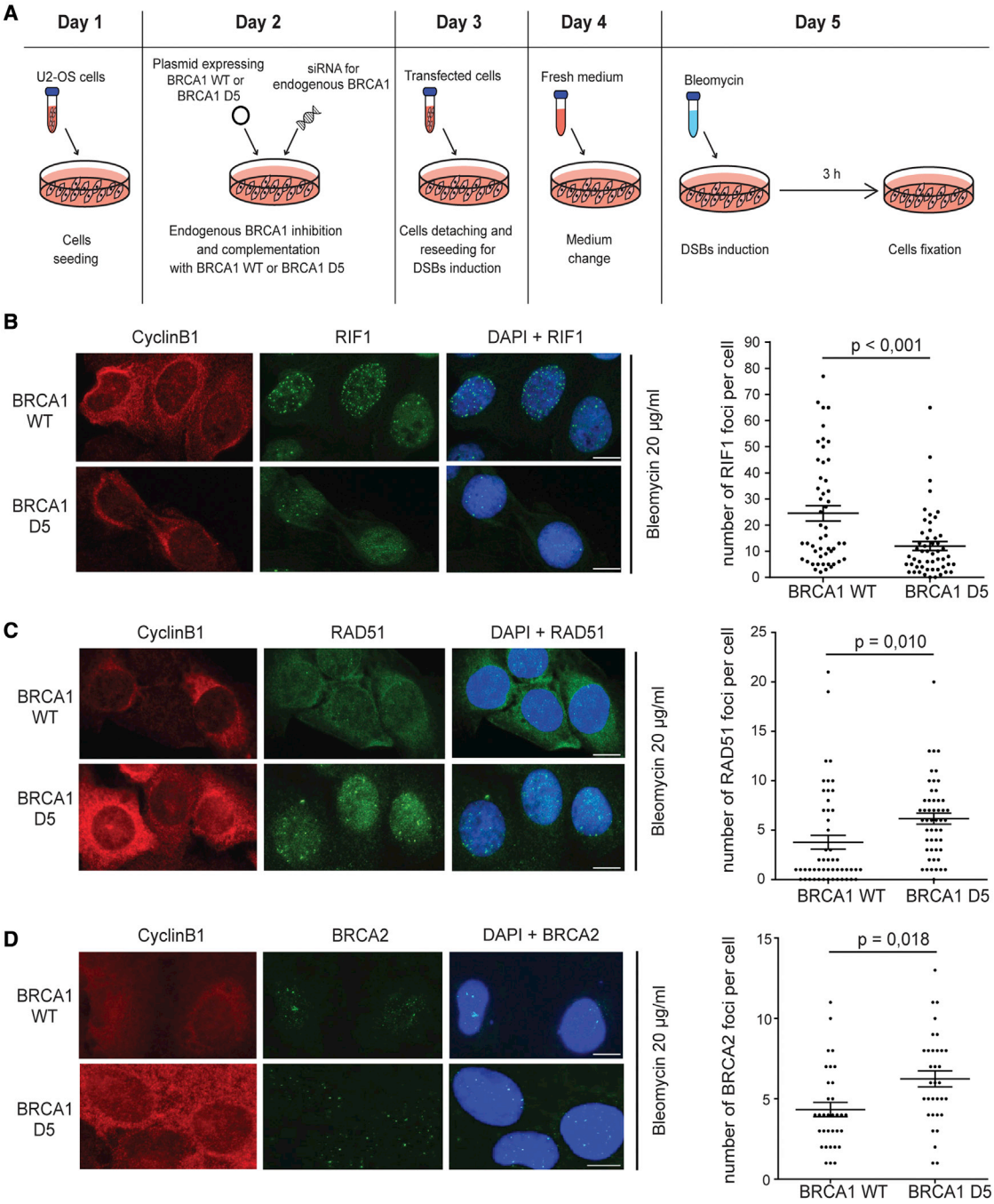

Figure 3. The expression of unPARylatable variant of BRCA1 reduces the recruitment at DSBs of the DNA resection inhibitor RIF1, while it increases the recruitment of the HR factors RAD51 and BRCA2

(A) Experimental pipeline for experiments in (B–D). U-2OS cells were co-transfected with a plasmid expressing BRCA1 (the WT or the variant D5) and siRNA2 to silence endogenous BRCA1, then cells were detached and seeded again. On day 5, they were treated for 3 h with bleomycin 20 μg/mL.

(B–D) Cells were fixed and analyzed by immunofluorescence microscopy to visualize RIF1 (B), RAD51 (C), or BRCA2 (D).

Ciclyn-B1 was analyzed to discriminate cells in S-G2 phase. Left: representative images of cells. Scale bars in all: 10 μm. Right: foci number per cell; a t test has been performed to analyze statistical difference between means calculated counting foci in at least 50 cells per experiment (n = 3, biologically independent experiments); p values obtained from this analysis are shown.

this, we quantified the amount of ssDNA formed by resection at Cas9-induced DSBs in cells ectopically expressing BRCA1-D5. To test the contribution of BRCA2 and EXO1, which was recently shown to be part of a complex with BRCA2 during resection,[21] we also performed the experiment in cells depleted of either BRCA2 or EXO1. The experiment workflow (Figure S4A) is similar to the one in Figure 3A, with the difference that BRCA2 or EXO1 have been silenced together with the endogenous BRCA1 and a BRCA1 gene copy is expressed from a plasmid. By this setting, BRCA1-D5 expression led to a statistically significant increase in DSB resection at longer distances from the cut site but not at shorter distances (Figure 4A). Moreover, treatment of BRCA1-D5 cells with olaparib did not result in an additive effect in ssDNA formation near the Cas9-induced DSBs (Figure S4B). These results show that BRCA1-D5 mutant partially phenocopies the effect of olaparib treatment on DSB resection; therefore, the increased ssDNA observed at distal region from the break with the drug strongly depends on a reduction of BRCA1 PARylation.

Considering the increased recruitment of BRCA2 at bleomycin-induced DSBs in cells expressing BRCA1-D5 (Figure 3D), we speculated that reducing PARylation of BRCA1 might foster DNA resection through the BRCA2-EXO1 axis.[22] Supporting this idea, the increased DSB resection of BRCA1-D5 cells was largely suppressed in cells depleted for BRCA2 or EXO1 (Figures 4B, 4C, S2, S4C, and S4D). Similar to what we observed in cells treated with olaparib (Figure 1), depletion of BRCA2 was accompanied by a slight increase of DSB2 resection, which was, however, not further elevated by expression of BRCA1-D5.

Consistent with its role as a resection barrier with RIF1 (revised in Marini et al.[10] and Ronato et al.[11]), 53BP1 limits nucleolytic processing of Cas9-induced DSBs.[26] Therefore, we hypothesized that the observed reduction of the 53BP1-RIF1 barrier (Figure 3B) could be the principal cause of the increased resection distal from the break site in BRCA1-D5 cells (Figure 4A). However, the depletion of 53BP1 in combination with the ectopic expression of BRCA1-D5 led to an additive increase in ssDNA far from the Cas9-induced DSBs (Figures 4D and S4E), suggesting that reducing BRCA1 PARylation triggers over-resection through a distinct mechanism rather than simply weakening the barrier by 53BP1-RIF1. Taking this observation together with the results obtained in BRCA2- and EXO1-depleted cells, we propose that BRCA1 PARylation might directly limit the BRCA2-EXO1 axis for resection.

DISCUSSION

The steric hindrance of PARP1 localized at DSBs was suggested to physically prevent the recruitment of EXO1 nuclease for DNA end resection.[23] Conversely, other evidence has shown that PARylation by PARP1 favors fast recruitment of EXO1 to DSBs induced by micro-laser irradiation.[21] It was shown that EXO1 localization depends on fast recruitment of BRCA2 to the damaged site via the BRCA2 oligonucleotide/oligosaccharide binding folds (OB folds) that mediate the interaction with PARylated targets.[21] However, both EXO1 and BRCA2 show a second step of retention at DSBs independent on PARylation,[21] likely reflecting dynamic interaction with several partners during the repair mechanism.

Remarkably, BRCA1 affinity to DNA is reduced upon PARylation by PARP1.[16] It has been shown that internal deletion of amino acid residues 611–618 (LRRKSSTR) in the BRCA1-D5 variant greatly reduces PARylation of other unknown sites of the protein, leading to a stronger binding to the DNA. Although the BRCA1-D5 variant interacts with important partner proteins, such as BARD1, CtIP, and BACH1, and shows nuclear localization and aggregation in foci in response to ionizing radiation,[16] cells expressing the BRCA1-D5 variant accumulate elevated aberrant recombination events, such as fusions/bridges, radial structures, and other complex chromosome rearrangements.[16] This hyper-recombination pattern in BRCA1-D5 cells depends on RAD51 and, partially, on EXO1 and DNA2, which mediate the long-range DSB resection.[16]

Here, based on the results obtained by ddPaD[26] and immunofluorescence analysis of RIF1 and RAD51 foci in response to the radiomimetic drug bleomycin, we propose that quickly after DSB formation, PARP1 PARylates BRCA1 and reduces its affinity to DNA, thus restraining DNA resection by limiting recruitment of BRCA2 and EXO1 to DSBs. Accordingly, the 53BP1-RIF1 barrier would not effectively counteract the resection machinery in BRCA1-D5 cells, which would ultimately accumulate gross chromosomal rearrangements and hyper-recombination events via RAD51.[16] Importantly, this model can explain results in cells treated with the PARP inhibitor olaparib for cancer therapy. Recently, olaparib has been approved to treat aggressive breast and ovarian cancers with mutations in BRCA1 or BRCA2 genes. As a proof of principle of the synthetic lethality approach,[29] the combination of BRCA1/BRCA2 deficiency and PARP inhibition kills cancer cells, causing an excessive accumulation of unrepaired DNA damage.[24,25] Moreover, mutations in separate genes leading to resistance to the therapy and/or cancer relapse have been frequently reported during treatment with olaparib. In *BRCA1*$^{-/-}$ or *BRCA2*$^{-/-}$ cells, typical mutations occur in genes controlling DSB resection, such as 53BP1,[24,25] restoring DSB processing and repair, although the mechanism is still poorly understood.

Here, we show that PARP1 inhibition by olaparib leads to over-resection of Cas9-induced DSBs, further supporting recent findings with talazoparib.[23] Interestingly, olaparib has lower DNA trapping activity than talazoparib,[30] suggesting that the PARP1 catalytic activity is more relevant to limit DSB resection than steric hindrance of the protein at the damaged site. More importantly, olaparib treatment does not induce over-resection of DSBs in cells depleted for BRCA1 or BRCA2. Conversely, PARP1 inhibition by talazoparib induces over-resection of ionizing radiation (IR)-induced DSBs in DLD1 *BRCA2*$^{-/-}$ cells.[23] This discrepancy can be due to different experimental setting and/or methodology to detect the ssDNA generated by resection. We also noticed that reducing global PARylation by olaparib has a more prominent effect than BRCA1-D5 mutation on DNA resection closer to the break site. This could be explained by other PARP1 targets playing roles in DSB processing. Consistent with this, PARP1 inhibition reduces the recruitment of the KU70/80 complex to DSB ends,[23] exposing DNA to the nucleolytic processing.[31]

Overall, our results have implications in clinical therapy. First, PARP inhibition might expose patients to the accumulation of aberrant chromosome rearrangements in healthy cells due to

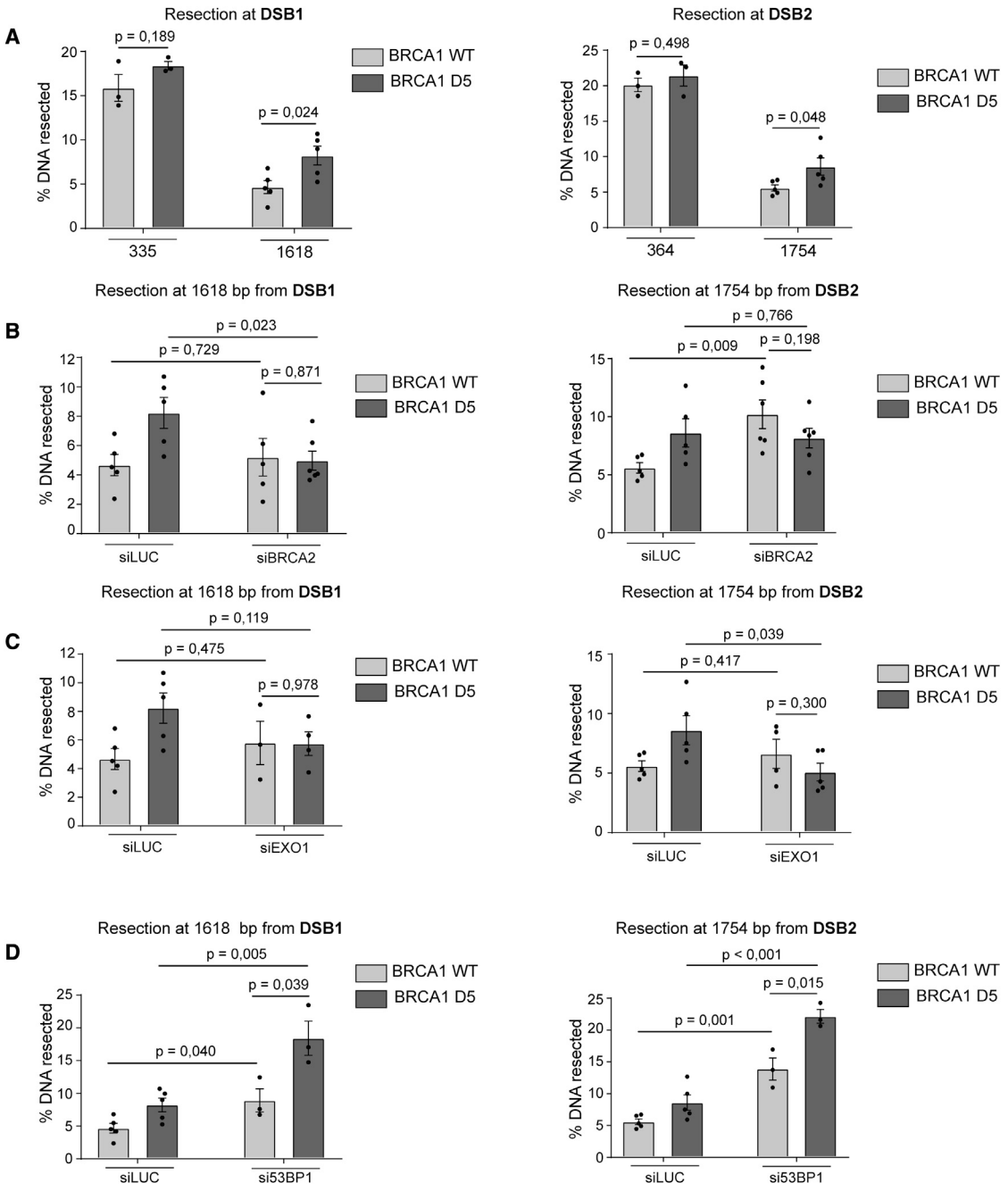

Figure 4. The expression of unPARylatable variant of BRCA1 triggers DNA hyper-resection at Cas9-induced DSB through BRCA2 and EXO1 synergistically with 53BP1 depletion

(A) Percentage of DNA resected at DSB1 and DSB2 by ddPCR analysis in U-2OS-SEC cells, expressing either wild type BRCA1 (WT) or the unPARylatable BRCA1-D5 variant, as described in Figure S4A.

(B–D) Same experiment as in (A) performed on cells silenced for BRCA2 (B), EXO1 (C), or 53BP1 (D).

All data are plotted as mean ± SEM; statistical difference was calculated using a t test to compare means calculated from at least three biological replicates; p values obtained from this analysis are shown. Data for siLUC are the same in (A)–(D) because the siRNA transfections targeting BRCA2, EXO1, or 53BP1 have been performed in parallel during the same experiment. Cut efficiency DSB1: siLUC (WT) = 53.50% ± 1.14%; siLUC (D5) = 51.27% ± 0.72%; siBRCA2 (WT) = 39.82% ± 0.68%; siBRCA2 (D5) = 44.37% ± 2.60%; siEXO1 (WT) = 38.57% ± 0.67%; siEXO (D5) = 43.61% ± 1.62%; si53BP1 (WT) = 54.13% ± 1.83%; si53BP1 (D5) = 56.56% ± 2.64%. Cut efficiency DSB2: siLUC (WT) = 43.26% ± 0.66%; siLUC (D5) = 42.37% ± 0.73%; siBRCA2 (WT) = 40.78% ± 2.17%; siBRCA2 (D5) = 42.68% ± 2.33%; siEXO1 (WT) = 35.94% ± 1.89%; siEXO (D5) = 40.34% ± 1.21%; si53BP1 (WT) = 52.74% ± 1.72%; si53BP1 (D5) = 54.57% ± 0.12%.

over-resection of spontaneous or therapy-induced DNA breaks. This risk should be taken into consideration and demands urgent investigation to develop strategies to monitor/reduce it. Second, the synthetic lethality induced by olaparib in *BRCA1*$^{-/-}$ or *BRCA2*$^{-/-}$ cells is not due to over-resection of DNA breaks. This elicits the chance to set up personalized therapy for patients with *BRCA*ness tumors, combining olaparib treatment with the administration of a specific compound designed to reinforce DSB resection barrier to protect healthy cells from unwanted illegitimate recombination events and genetic instability caused by olaparib treatment.

Limitations of the study

In our experimental conditions, we showed that HPF1 is important for RIF1 and RAD51 foci metabolism, but we did not provide proof that HPF1 cooperates with PARP1 for BRCA1 PARylation. This would be a challenge because HPF1-dependent serine mono ADP-ribosylation of BRCA1 may be involved in regulatory network of mutual exclusive phosphorylation and PARylation of the same serine residues of BRCA1, as well as other factors. It will be interesting to define whether hypo-PARylation of certain serine residues of BRCA1 (e.g., Ser-308, which is either phosphorylated by AURKA[32] or mono ADP-ribosylated by PARP1 in response to DNA damage[4,17]) is associated with an increased level of serine phosphorylation, which could be potentially implicated in DSB processing and repair.[33–39] Further characterization of BRCA1 serine residues will be informative to dissect the complete regulatory network played by phosphorylation and PARylation of BRCA1. Indeed, here we took advantage of the BRCA1-D5 variant, which, however, does not carry a mutation at specific PARylation sites.

STAR★METHODS

Detailed methods are provided in the online version of this paper and include the following:

- KEY RESOURCES TABLE
- RESOURCE AVAILABILITY
  - Lead contact
  - Material availability
  - Data and code availability
- EXPERIMENTAL MODEL AND SUBJECT DETAILS
- METHOD DETAILS
  - Cell silencing and drug treatment
  - BRCA1 unPARylatable variant-complemented cell treatment
  - Human genomic DNA extraction and restriction digestion
  - DNA resection analysis
  - Protein extraction
  - Western blot
  - Immunofluorescence
- QUANTIFICATION AND STATISTICAL ANALYSIS

SUPPLEMENTAL INFORMATION

Supplemental information can be found online at https://doi.org/10.1016/j.celrep.2023.112060.

ACKNOWLEDGMENTS

We thank David Livingston for generously providing the plasmid DNA to express the BRCA1-WT and BRCA1-D5 alleles. We thank Laura Caleca for technical support with BRCA2 immunofluorescence and Pablo Huertas for the CtIP antibody. We thank Alvaro Monteiro for reading the paper. We are grateful to all the members of our laboratories for helpful discussions. This work was supported by grants from Associazione Italiana Ricerca sul Cancro (AIRC_IG19917 to A.P.). S.L. was supported by a fellowship from Fondazione Veronesi.

AUTHOR CONTRIBUTIONS

Conceptualization, S.L., R.Q., S.S., and A.P.; investigation, S.L., R.Q., and S.S.; writing – original draft, S.L., R.Q., S.S., and A.P.; writing – review & editing, S.L., R.Q., S.S., and A.P.; funding acquisition, A.P.; supervision, A.P.

DECLARATION OF INTERESTS

The authors declare no competing interests.

Received: September 14, 2022
Revised: November 23, 2022
Accepted: January 18, 2023
Published: February 1, 2023

REFERENCES

1. Gibson, B.A., and Kraus, W.L. (2012). New insights into the molecular and cellular functions of poly(ADP-ribose) and PARPs. Nat. Rev. Mol. Cell Biol. *13*, 411–424. https://doi.org/10.1038/nrm3376.
2. Liu, C., Vyas, A., Kassab, M.A., Singh, A.K., and Yu, X. (2017). The role of poly ADP-ribosylation in the first wave of DNA damage response. Nucleic Acids Res. *45*, 8129–8141. https://doi.org/10.1093/NAR/GKX565.
3. Leidecker, O., Bonfiglio, J.J., Colby, T., Zhang, Q., Atanassov, I., Zaja, R., Palazzo, L., Stockum, A., Ahel, I., and Matic, I. (2016). Serine is a new target residue for endogenous ADP-ribosylation on histones. Nat. Chem. Biol. *12*, 998–1000. https://doi.org/10.1038/NCHEMBIO.2180.
4. Larsen, S.C., Hendriks, I.A., Lyon, D., Jensen, L.J., and Nielsen, M.L. (2018). Systems-wide analysis of serine ADP-ribosylation reveals widespread occurrence and site-specific overlap with phosphorylation. Cell Rep. *24*, 2493–2505.e4. https://doi.org/10.1016/J.CELREP.2018.07.083.
5. Palazzo, L., Leidecker, O., Prokhorova, E., Dauben, H., Matic, I., and Ahel, I. (2018). Serine is the major residue for ADP-ribosylation upon DNA damage. Elife *7*, e34334. https://doi.org/10.7554/ELIFE.34334.
6. Hendriks, I.A., Larsen, S.C., and Nielsen, M.L. (2019). An advanced strategy for comprehensive profiling of ADP-ribosylation sites using mass spectrometry-based proteomics. Mol. Cell. Proteomics *18*, 1010–1026. https://doi.org/10.1074/MCP.TIR119.001315.
7. Buch-Larsen, S.C., Hendriks, I.A., Lodge, J.M., Rykær, M., Furtwängler, B., Shishkova, E., Westphall, M.S., Coon, J.J., and Nielsen, M.L. (2020). Mapping physiological ADP-ribosylation using activated ion electron transfer dissociation. Cell Rep. *32*, 108176. https://doi.org/10.1016/J.CELREP.2020.108176.
8. Bonfiglio, J.J., Fontana, P., Zhang, Q., Colby, T., Gibbs-Seymour, I., Atanassov, I., Bartlett, E., Zaja, R., Ahel, I., and Matic, I. (2017). Serine ADP-ribosylation depends on HPF1. Mol. Cell *65*, 932–940.e6. https://doi.org/10.1016/J.MOLCEL.2017.01.003.
9. Cejka, P., and Symington, L.S. (2021). DNA end resection: mechanism and control. Annu. Rev. Genet. *55*, 285–307. https://doi.org/10.1146/ANNUREV-GENET-071719-020312.
10. Marini, F., Rawal, C.C., Liberi, G., and Pellicioli, A. (2019). Regulation of DNA double strand breaks processing: focus on barriers. Front. Mol. Biosci. *6*, 55. https://doi.org/10.3389/fmolb.2019.00055.

11. Ronato, D.A., Mersaoui, S.Y., Busatto, F.F., Affar, E.B., Richard, S., and Masson, J.-Y. (2020). Limiting the DNA double-strand break resectosome for genome protection. Trends Biochem. Sci. *45*, 779–793. https://doi.org/10.1016/j.tibs.2020.05.003.

12. Myler, L.R., and Finkelstein, I.J. (2017). Eukaryotic resectosomes: a single-molecule perspective. Prog. Biophys. Mol. Biol. *127*, 119–129. https://doi.org/10.1016/j.pbiomolbio.2016.08.001.

13. Symington, L.S. (2016). Mechanism and regulation of DNA end resection in eukaryotes. Crit. Rev. Biochem. Mol. Biol. *51*, 195–212. https://doi.org/10.3109/10409238.2016.1172552.

14. Zhao, W., Wiese, C., Kwon, Y., Hromas, R., and Sung, P. (2019). The BRCA tumor suppressor network in chromosome damage repair by homologous recombination. Annu. Rev. Biochem. *88*, 221–245. https://doi.org/10.1146/annurev-biochem-013118-111058.

15. Chen, C.-C., Feng, W., Lim, P.X., Kass, E.M., and Jasin, M. (2018). Homology-directed repair and the role of BRCA1, BRCA2, and related proteins in genome integrity and cancer. Annu. Rev. Cancer Biol. *2*, 313–336. https://doi.org/10.1146/annurev-cancerbio-030617-050502.

16. Hu, Y., Petit, S.A., Ficarro, S.B., Toomire, K.J., Xie, A., Lim, E., Cao, S.A., Park, E., Eck, M.J., Scully, R., et al. (2014). PARP1-driven poly-ADP-ribosylation regulates BRCA1 function in homologous recombination-mediated DNA repair. Cancer Discov. *4*, 1430–1447. https://doi.org/10.1158/2159-8290.CD-13-0891.

17. Hendriks, I.A., Buch-Larsen, S.C., Prokhorova, E., Elsborg, J.D., Rebak, A.K.L.F.S., Zhu, K., Ahel, D., Lukas, C., Ahel, I., and Nielsen, M.L. (2021). The regulatory landscape of the human HPF1- and ARH3-dependent ADP-ribosylome. Nat. Commun. *12*, 5893. https://doi.org/10.1038/S41467-021-26172-4.

18. Yang, G., Chen, Y., Wu, J., Chen, S.-H., Liu, X., Singh, A.K., and Yu, X. (2020). Poly(ADP-ribosyl)ation mediates early phase histone eviction at DNA lesions. Nucleic Acids Res. *48*, 3001–3013. https://doi.org/10.1093/nar/gkaa022.

19. Haince, J.-F., McDonald, D., Rodrigue, A., Déry, U., Masson, J.-Y., Hendzel, M.J., and Poirier, G.G. (2008). PARP1-dependent kinetics of recruitment of MRE11 and NBS1 proteins to multiple DNA damage sites. J. Biol. Chem. *283*, 1197–1208. https://doi.org/10.1074/jbc.M706734200.

20. Li, M., Lu, L.-Y., Yang, C.-Y., Wang, S., and Yu, X. (2013). The FHA and BRCT domains recognize ADP-ribosylation during DNA damage response. Genes Dev. *27*, 1752–1768. https://doi.org/10.1101/gad.226357.113.

21. Zhang, F., Shi, J., Bian, C., and Yu, X. (2015). Poly(ADP-Ribose) mediates the BRCA2-dependent early DNA damage response. Cell Rep. *13*, 678–689. https://doi.org/10.1016/j.celrep.2015.09.040.

22. Zhang, F., Shi, J., Chen, S.-H., Bian, C., and Yu, X. (2015). The PIN domain of EXO1 recognizes poly(ADP-ribose) in DNA damage response. Nucleic Acids Res. *43*, 10782–10794. https://doi.org/10.1093/nar/gkv939.

23. Caron, M.-C., Sharma, A.K., O'Sullivan, J., Myler, L.R., Ferreira, M.T., Rodrigue, A., Coulombe, Y., Ethier, C., Gagné, J.P., Langelier, M.-F., et al. (2019). Poly(ADP-ribose) polymerase-1 antagonizes DNA resection at double-strand breaks. Nat. Commun. *10*, 2954. https://doi.org/10.1038/s41467-019-10741-9.

24. D'Andrea, A.D. (2018). Mechanisms of PARP inhibitor sensitivity and resistance. DNA Repair *71*, 172–176. https://doi.org/10.1016/j.dnarep.2018.08.021.

25. Slade, D. (2020). PARP and PARG inhibitors in cancer treatment. Genes Dev. *34*, 360–394. https://doi.org/10.1101/gad.334516.119.

26. Dibitetto, D., La Monica, M., Ferrari, M., Marini, F., and Pellicioli, A. (2018). Formation and nucleolytic processing of Cas9-induced DNA breaks in human cells quantified by droplet digital PCR. DNA Repair *68*, 68–74. https://doi.org/10.1016/j.dnarep.2018.06.005.

27. Gomez-Cabello, D., Jimeno, S., Fernández-Ávila, M.J., and Huertas, P. (2013). New tools to study DNA double-strand break repair pathway choice. PLoS One *8*, e77206. https://doi.org/10.1371/journal.pone.0077206.

28. Smith, R., Zentout, S., Chapuis, C., Timinszky, G., and Huet, S. (2021). HPF1-dependent histone ADP-ribosylation triggers chromatin relaxation to promote the recruitment of repair factors at sites of DNA damage. Preprint at bioRxiv. https://doi.org/10.1101/2021.08.27.457930.

29. Lord, C.J., and Ashworth, A. (2017). PARP inhibitors: synthetic lethality in the clinic. Science *355*, 1152–1158. https://doi.org/10.1126/science.aam7344.

30. Pommier, Y., O'Connor, M.J., and de Bono, J. (2016). Laying a trap to kill cancer cells: PARP inhibitors and their mechanisms of action. Sci. Transl. Med. *8*, 362ps17. https://doi.org/10.1126/scitranslmed.aaf9246.

31. Myler, L.R., Gallardo, I.F., Soniat, M.M., Deshpande, R.A., Gonzalez, X.B., Kim, Y., Paull, T.T., and Finkelstein, I.J. (2017). Single-Molecule imaging reveals how mre11-rad50-Nbs1 initiates DNA break repair. Mol. Cell *67*, 891–898.e4. https://doi.org/10.1016/j.molcel.2017.08.002.

32. Ertych, N., Stolz, A., Valerius, O., Braus, G.H., and Bastians, H. (2016). CHK2-BRCA1 tumor-suppressor axis restrains oncogenic Aurora-A kinase to ensure proper mitotic microtubule assembly. Proc. Natl. Acad. Sci. USA. *113*, 1817–1822. https://doi.org/10.1073/PNAS.1525129113.

33. Cortez, D., Wang, Y., Qin, J., and Elledge, S.J. (1999). Requirement of ATM-dependent phosphorylation of brca1 in the DNA damage response to double-strand breaks. Science *286*, 1162–1166. https://doi.org/10.1126/SCIENCE.286.5442.1162.

34. Beckta, J.M., Dever, S.M., Gnawali, N., Khalil, A., Sule, A., Golding, S.E., Rosenberg, E., Narayanan, A., Kehn-Hall, K., Xu, B., et al. (2015). Mutation of the BRCA1 SQ-cluster results in aberrant mitosis, reduced homologous recombination, and a compensatory increase in non-homologous end joining. Oncotarget *6*, 27674–27687. https://doi.org/10.18632/ONCOTARGET.4876.

35. Xu, B., Kim, S., and Kastan, M.B. (2001). Involvement of Brca1 in S-phase and G(2)-phase checkpoints after ionizing irradiation. Mol. Cell Biol. *21*, 3445–3450. https://doi.org/10.1128/MCB.21.10.3445-3450.2001.

36. Johnson, N., Cai, D., Kennedy, R.D., Pathania, S., Arora, M., Li, Y.C., D'Andrea, A.D., Parvin, J.D., and Shapiro, G.I. (2009). Cdk1 participates in BRCA1-dependent S phase checkpoint control in response to DNA damage. Mol. Cell *35*, 327–339. https://doi.org/10.1016/J.MOLCEL.2009.06.036.

37. Chabalier-Taste, C., Brichese, L., Racca, C., Canitrot, Y., Calsou, P., and Larminat, F. (2016). Polo-like kinase 1 mediates BRCA1 phosphorylation and recruitment at DNA double-strand breaks. Oncotarget *7*, 2269–2283. https://doi.org/10.18632/ONCOTARGET.6825.

38. Qi, L., Chakravarthy, R., Li, M.M., Deng, C.X., Li, R., and Hu, Y. (2022). Phosphorylation of BRCA1 by ATM upon double-strand breaks impacts ATM function in end-resection: a potential feedback loop. iScience *25*, 104944. https://doi.org/10.1016/J.ISCI.2022.104944.

39. Xu, B., O'Donnell, A.H., Kim, S.-T., and Kastan, M.B. (2002). Phosphorylation of serine 1387 in Brca1 is specifically required for the Atm-mediated S-phase checkpoint after ionizing irradiation. Cancer Res. *62*, 4588–4591.

40. Muñoz, M.C., Yanez, D.A., and Stark, J.M. (2014). An RNF168 fragment defective for focal accumulation at DNA damage is proficient for inhibition of homologous recombination in BRCA1 deficient cells. Nucleic Acids Res. *42*, 7720–7733. https://doi.org/10.1093/nar/gku421.

41. Park, H.J., Bae, J.S., Kim, K.M., Moon, Y.J., Park, S.-H., Ha, S.H., Hussein, U.K., Zhang, Z., Park, H.S., Park, B.-H., et al. (2018). The PARP inhibitor olaparib potentiates the effect of the DNA damaging agent doxorubicin in osteosarcoma. J. Exp. Clin. Cancer Res. *37*, 107. https://doi.org/10.1186/s13046-018-0772-9.

STAR★METHODS

KEY RESOURCES TABLE

REAGENT or RESOURCE	SOURCE	IDENTIFIER
Antibodies		
Mouse anti-human BRCA1 antibody [8F7]	Genetex	GTX70113; RRID: AB_368614
Mouse anti-human BRCA2 antibody (3D12)	Santa-Cruz	SC-293185
Goat anti-human BRCA2 antibody (C19)	Santa-Cruz	SC-1817; RRID: AB_630948
Rabbit anti-human 53BP1 antibody	Cell Signaling	4937; RRID: AB_10694558
Rabbit anti-human EXO1 antibody	Sigma-Aldrich	SAB4503568; RRID: AB_10761635
Rabbit anti-human Poly/Mono-ADP Ribose (PAR) (E6F6A) antibody	Cell Signaling	83732; RRID: AB_2749858
Rabbit anti-human RIF1 antibody	Thermo Fischer Scientific	PA5-57857; RRID: AB_2646559
Rabbit anti-human RAD51 antibody (Ab-1)	Calbiochem	PC-130; RRID: AB_2238184
Mouse anti-human CYCLIN-B1 antibody	BD pharmingen	554176; RRID: AB_395287
Rabbit anti-human HPF1 antibody	Sigma-Aldrich	HPA043467; RRID: AB_10793949
Mouse anti-human CtIP antibody	Active Motif	61141; RRID: AB_2714164
Bacterial and virus strains		
DH5alpha competent cells	Thermo Fisher Scientific	18,265,017
Chemicals, peptides, and recombinant proteins		
Doxycycline	Merck	D9891
Bleomycin	Merck	B7216
Penicillin-Streptomycin	Euroclone	ECB3001
Hygromycin	Genespin®	STS-HY1
Blasticidine	Genespin®	STS-BLAS20
Formaldehyde	Sigma-Aldrich	P6148
Olaparib (AZD2281)	Selleckchem	S1060
BsrGI-HF®	NEB	R3575S
BamHI-HF®	NEB	R3136S
ddPCR Supermix for Probes (No dUTP)	Bio-Rad	1,863,025
cOmplete™ ULTRA Tablets, Mini, Protease Inhibitor Cocktail	Roche	5,892,970,001
Proteinase K	Amsbio	120,493–1
RNase A	Sigma-Aldrich	R6513
ProlongGold with DAPI	Thermo Fischer Scientific	P36931
Leica immersion oil type F	Thermo Fischer Scientific	11,944,399
Critical commercial assays		
Qiagen Spin Miniprep Kit	Qiagen	27,106
Lipofectamine RNAiMAX Transfection Reagent	Thermo Fischer Scientific	13,778,150
Lipofectamine 2000 Transfection Reagent	Thermo Fischer Scientific	11,668,019
NucleoSpin Tissue, Mini kit for DNA from cells and tissue	Macherey-Nagel	740,952.250
NuPAGE™ 4 to 12%, Bis-Tris, 1.5 mm, 10-well	Thermo Fischer Scientific	NP0335PK2
Clarity Western ECL Substrate	Biorad	1,705,061
Droplet Generation Oil for Probes	Biorad	1,863,005
Droplet generator gasket	Biorad	1,863,009
Droplet Generator cartridge	Biorad	1,864,008

(*Continued on next page*)

Continued

REAGENT or RESOURCE	SOURCE	IDENTIFIER
Experimental models: Cell lines		
Human: U2OS Stably Expressing Cas9	Munoz et al.[40]	N/A
Oligonucleotides		
For list of oligonucleotides, see Table S1	N/A	N/A
Recombinant DNA		
pcDNA3-BRCA1WT-HA	Hu et al.[16]	N/A
pcDNA3-BRCA1D5-HA	Hu et al.[16]	N/A
Software and algorithms		
ImageJ	NIH	https://ImageJ.nih.gov
Image Lab	Bio-Rad	https://www.bio-rad.com
Graph-pad Prism 7	Graphpad.com	https://www.graphpad.com
Other		
Biorad CFX Connect	Bio-Rad	https://www.bio-rad.com
Biorad Droplet Digital PCR	Bio-Rad	https://www.bio-rad.com
Leica DMRA2 Microscope	Leica	https://www.leica-microsystems.com
Leica FW4000 software	Leica	https://www.leica-microsystems.com

RESOURCE AVAILABILITY

Lead contact

Further information and request for resources and reagents should be directed and will be fulfilled by the lead contact, Dr. Achille Pellicioli (achille.pellicioli@unimi.it).

Material availability

The unique reagents generated in this study are available from the lead contact upon request.

Data and code availability

- All data reported in this paper will be shared by the lead contact upon request.
- This paper does not report original code.
- Any additional information required to reanalyze the data reported in this paper is available from the lead contact upon request.

EXPERIMENTAL MODEL AND SUBJECT DETAILS

U-2OS-SEC (Human osteosarcoma Stably Expressing Cas9, under the tetracycline-inducible element) cells were available from Professor John Rouse (https://mrcppureagents.dundee.ac.uk), and were grown in Dulbecco's Modified Eagle Medium (DMEM; Gibco) containing 10% Fetal Bovine Serum (FBS; Gibco) and 1% Penicillin/Streptomycin (Euroclone). Selection has been maintained adding hygromycin 100 μg/mL and blasticidine 15 μg/mL to grow medium. They were incubated at 37°C at 5% CO2 in air atmosphere in a suitable incubator. SpCas9 was induced with 1 μg/mL doxycycline for 24 h before sgRNAs transfection.

METHOD DETAILS

Cell silencing and drug treatment

For silencing experiments siRNAs used are listed in Table S1; silencing was obtained transfecting cell line with Lipofectamine RNAiMAX (Invitrogen) according to the manufacturer's instructions.

For Olaparib (PARP1 inhibitor) treatment, the drug stock was created in DMSO at a concentration of 1mM and it was used at a final concentration of 5μM diluted directly in cell medium. Olaparib concentration has been decided based on literature analysis and experimental tests.[41] For DNA resection experiments, Olaparib was administered for 4.5 h, starting from 1.5 h after sgRNA-mediated DSBs induction. For immunofluorescence experiments, it was administered for 3 h simultaneously with Bleomycin-mediated DSBs induction.

BRCA1 unPARylatable variant-complemented cell treatment

For resection experiments in BRCA1 complemented cell lines, cells were first transfected with plasmid expressing either BRCA1 WT or BRCA1-D5, siRNA against endogenous BRCA1 (siRNA2 BRCA1) and another siRNA where needed (siBRCA2, si53BP1 or siEXO1)

using Lipofectamine 2000 (Invitrogen) according to the manufacturer's instructions. After 24 h, cells were trypsinized and seeded in 12-wells plates for Cas9 induction and sgRNAs transfection. The next day, Cas9 is induced for 24 h and then (72 h after plasmid and siRNA transfection) DSB1 and DSB2 were induced with sgRNAs transfection, for 6 h.

For immunofluorescence experiments in BRCA1 complemented cell lines, cells were first transfected with plasmid expressing either BRCA1 WT or BRCA1-D5 and siRNA against endogenous BRCA1 (siRNA2 BRCA1) using Lipofectamine 2000 protocol. The day after cells were trypsinized, seeded in 24-wells plates directly on glass coverslips and 72 h after plasmid and siRNA transfection, DSBs are induced with bleomycin (20μg/mL) for 3 h.

Human genomic DNA extraction and restriction digestion

U-2OS-SEC were grown on 12-well plates after transfection. At the indicated time points, cells where trypsinized, washed in PBS and genomic DNA was extracted by NucleoSpin™ Tissue kit (Macherey-Nagel), according to the manufacturer's instructions. The day after, 15μL of genomic DNA (DNA concentration is around 100 ng/μL) were digested or mock with 20 units of BsrGI or BamHI restriction enzymes (New England BioLabs) for 4 h at 37°C. 5μL of digested or mock DNA were used for the ddPCR reaction for resection analysis.

DNA resection analysis

ddPCR resection analysis was performed as described in.[26] Briefly, 5μL of genomic DNA, 1X ddPCR™ Supermix for Probes (no dUTP, Bio-Rad), 900nM for each pair of primers, 250nM for each probe (HEX and FAM, TaqMan probes) and dH2O to 20μL per sample are used to produce droplets with a droplet generator (QX200™, Bio-Rad). 40μL of emulsion were transferred to a 96-well ddPCR plate and PCR reaction were performed.

Cut efficiency (CE) was calculated with the following formula:

$$CE = \left(1 - \left(r_{+\,\mathrm{sgRNA}} \,/\, r_{-\,\mathrm{sgRNA}}\right)\right) * 100$$

Where r is the ratio between the number of copies of the locus across the Cas9 sites (HEX1 and HEX2 across probes) and a control locus on Chr. 22 (No-DSB FAM probe) in cells transfected with or without sgRNAs.

For the measurement of ssDNA generated by the resection process (SS), we calculated the ratio (r) between the number of copies nearby the DSB loci (for proximal probes 335 bp from DSB1 and 364 bp from DSB2, recognized by HEX3 and HEX4 probes respectively, for distal probes 1624 bp from DSB1 and 1712 from DSB2, recognized by HEX5 and HEX6 probes respectively) and a control nontarget locus (NT locus) on Chr. 22 (No-DSB FAM probe), with or without sgRNA, digested or mock with *Bsr*GI or *Bam*HI restriction enzymes. The absolute percentage of ssDNA was then calculated with the following equation:

$$SS = \left[\left(r_{\mathrm{digested}}/r_{\mathrm{mock}}\right)_{+\,\mathrm{sgRNA}} - \left(r_{\mathrm{digested}}/r_{\mathrm{mock}}\right)_{-\,\mathrm{sgRNA}}\right] * 100$$

Finally, resection value (RES) is calculated by the following formula:

$$\mathrm{RES} = \mathrm{SS}/\mathrm{CE}$$

All the sequences of primers and probes used are listed in Table S1.

Protein extraction

Proteins were extracted by resuspending cells pellet in 15μL of SDS 5% and boiling them at 95° for 10 min. Then, another volume of SDS 5% is added together with protease inhibitor (PMSF) and phosphatases inhibitor (PIC2 and PIC3). Finally, samples are sonicated for 25 s and quantified with microBCA (Euroclone®) protocol, following the manufacturer's instructions.

Western blot

For Western blot 30μg of proteins per sample analyzed were run on poly-acrylamide precast gel 4-12% (Bio-Rad) for 2 h at 120V. Afterward, proteins were transferred to nitrocellulose membrane and blotted with specific primary antibodies for 24 h at 4°. The next day, secondary antibodies were applied for 1 h at room temperature and proteins signal was evaluated with chemiluminescence reaction using a chemidoc (Bio-Rad).

Immunofluorescence

Three hours after DSBs induction with bleomycin, cells were washed once with PBS and fixed with paraformaldehyde (4%) for 15 min at RT, then washed again with PBS and stored at 4°C for 24h.

The day after, cells were treated with permeabilization buffer (PBS/Triton X-(0.1%)) for 3 min and washed with PBS for 5 min, afterward cells were treated with blocking solution (PBS/BSA (3%)) for 30 min. After blocking, primary antibodies are added to each well for 3h and then fluorescence AlexaFluor secondary antibodies for 1h with opportune emission wavelengths. All antibodies were diluted in PBS/BSA (1%). Lastly, glass coverslips are positioned on glass slides with a drop of DAPI per coverslip on it and analyzed with a fluorescence microscope (Leica).

QUANTIFICATION AND STATISTICAL ANALYSIS

Data are expressed as ± standard error of the mean (SEM) unless otherwise stated. Statistical tests were performed using the Student's t-test using Graph-pad Prism 7. p values were determined by an unpaired two-tailed t test. No statistical methods or criteria were used to estimate sample size or to include or exclude samples.